JACS
JOURNAL OF THE AMERICAN CHEMICAL SOCIETY
pubs.acs.org/JACS
Article

Scope and Mechanistic Probe into Asymmetric Synthesis of α-Trisubstituted-α-Tertiary Amines by Rhodium Catalysis

Madhawee K. Arachchi, Richard N. Schaugaard, H. Bernhard Schlegel,* and Hien M. Nguyen*

Cite This: J. Am. Chem. Soc. 2023, 145, 19642−19654
Read Online

ABSTRACT: Asymmetric reactions that convert racemic mixtures into enantioenriched amines are of significant importance due to the prevalence of amines in pharmaceuticals, with about 60% of drug candidates containing tertiary amines. Although transition-metal catalyzed allylic substitution processes have been developed to provide access to enantioenriched α-disubstituted allylic amines, enantioselective synthesis of sterically demanding α-tertiary amines with a tetrasubstituted carbon stereocenter remains a major challenge. Herein, we report a chiral diene-ligated rhodium-catalyzed asymmetric substitution of racemic tertiary allylic trichloroacetimidates with aliphatic secondary amines to afford α-trisubstituted-α-tertiary amines. Mechanistic investigation is conducted using synergistic experimental and computational studies. Density functional theory calculations show that the chiral diene-ligated rhodium promotes the ionization of tertiary allylic substrates to form both *anti* and *syn* π-allyl intermediates. The *anti* π-allyl pathway proceeds through a higher energy than the *syn* π-allyl pathway. The rate of conversion of the less reactive π-allyl intermediate to the more reactive isomer via π−σ−π interconversion was faster than the rate of nucleophilic attack onto the more reactive intermediate. These data imply that the Curtin−Hammett conditions are met in the amination reaction, leading to dynamic kinetic asymmetric transformation. Computational studies also show that hydrogen bonding interactions between β-oxygen of allylic substrate and amine-NH greatly assist the delivery of amine nucleophile onto more hindered internal carbon of the π-allyl intermediate. The synthetic utility of the current methodology is showcased by efficient preparation of α-trisubstituted-α-tertiary amines featuring pharmaceutically relevant secondary amine cores with good yields and excellent selectivities (branched−linear >99:1, up to 99% enantiomeric excess).

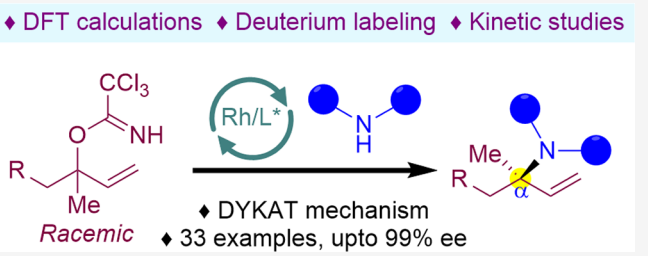

INTRODUCTION

Chiral amines are valuable building blocks in pharmaceuticals and naturally occurring alkaloids.[1,2] It is estimated that at least 80% of small molecule pharmaceuticals feature an amine moiety, and 60% of those are tertiary amines.[2−4] The ubiquitous presence of amines in biologically relevant molecules ascribes to their unique physiochemical properties. Besides their inherent ability to participate in hydrogen bonding with target receptors, amines could exist in the protonated form, which is critically important for binding potency at the target. Substituents on the nitrogen atom of amines also impact lipophilicity and membrane permeability, thus providing a synthetic handle to tune ADME (absorption, distribution, metabolism, and excretion) properties.[5] Therefore, robust and efficient protocols for the synthesis of chiral amines are an important endeavor. In particular, α-tertiary amines bearing a chiral quaternary carbon are an attractive class of bioactive molecules (Figure 1) and privileged ligands in asymmetric catalysis.[6,7]

Owing to the importance of α-tertiary amines and chiral amines containing α-trisubstituted carbon, several efficient methodologies have been developed to construct these motifs including 1,2-addition to ketimines,[8,9] hydroamination of alkenes and dienes,[10−16] C−H amination,[17,18] molecular rearrangements,[19] photocatalysis,[20,21] and biocatalysis.[22] Recently, major breakthroughs independently reported by the White[17] and Jiang[18] groups unveiled palladium-catalyzed oxidative amination of variety of olefins with aliphatic secondary amines leading to linear α-tertiary allylic amines lacking a stereocenter (Figure 2A). The Gevorgyan group was subsequently able to circumvent this regioselective bias to afford branched α-tertiary amines in asymmetric fashion (Figure 2A).[23]

Despite these major discoveries, reactions of racemic mixtures with aliphatic secondary amines to form enantioenriched α-trisubstituted-α-tertiary amines remain underdeveloped (Figure 2B).[24] We define an α-trisubstituted α-tertiary amine as a nitrogen atom is bound to an sp^3-tetrasubstituted

Received: April 23, 2023
Published: August 31, 2023

https://doi.org/10.1021/jacs.3c04211
J. Am. Chem. Soc. 2023, 145, 19642−19654

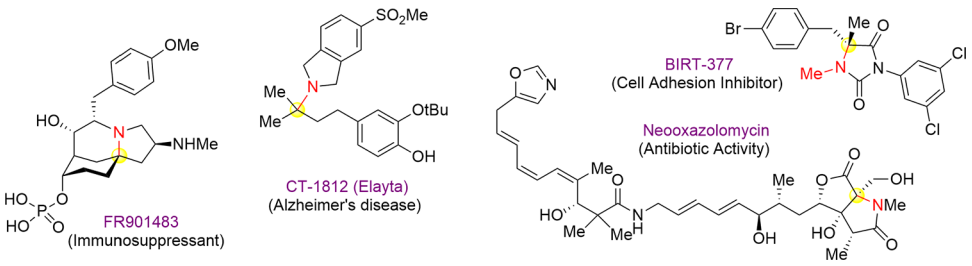

Figure 1. Bioactive molecules containing α-trisubstituted α-tertiary amines.

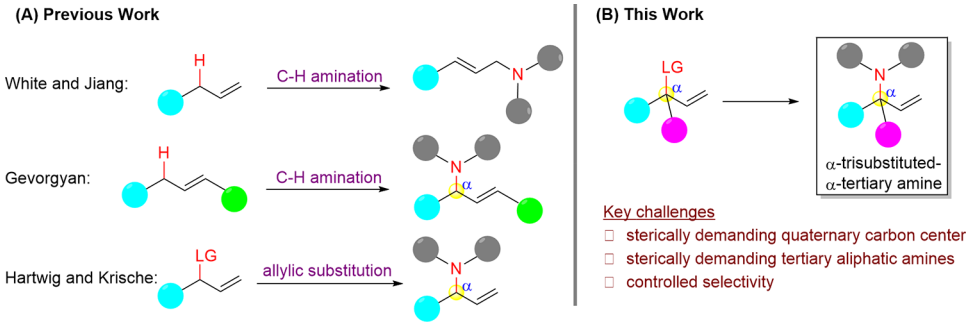

Figure 2. (A) Regioselective synthesis of linear α-tertiary amines and asymmetric synthesis of α-disubstituted-α-tertiary amines. (B) Asymmetric synthesis of α-trisubstituted-α-tertiary amines.

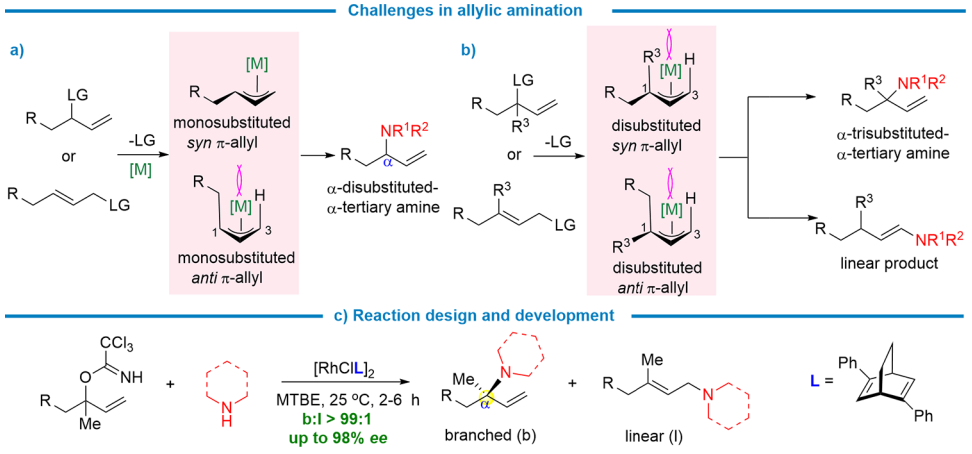

Figure 3. (a) Transition-metal-catalyzed enantioselective synthesis of α-disubstituted-α-tertiary amines. (b) Challenges associated with enantioselective synthesis of α-trisubstituted-α-tertiary amines. (c) Reaction design and development.

carbon. In turn, nitrogen could be sp^3-hybridized bearing three substituents. Altogether, α-trisubstituted α-tertiary amines can bear five substituents enhancing the chemical space to modulate molecular topology in drug-based discovery. However, construction of this scaffold is challenging because of highly substituted carbon and nitrogen centers (Figure 2B). Controlling enantioselectivity, wherein a carbon atom is chiral, further elevates this challenge.[25−28]

Transition metal-catalyzed asymmetric allylic substitution is a powerful and reliable tool to incorporate α-chiral amine into organic molecules.[29,30] The Hartwig[31,32] and Krische[33,34] groups have illustrated asymmetric syntheses of α-disubstituted α-tertiary amines starting from either linear or branched secondary allylic electrophiles and secondary aliphatic amines (Figures 2A and 3a). On the other hand, allylation of aliphatic secondary amines to form α-trisubstituted α-tertiary amines remains untapped likely because of challenges associated with controlling the selectivity of highly substituted C−N bond formation (Figure 3b).[35] In transition metal-catalyzed allylic substitution, the reaction proceeds through π-allyl intermediates which could exist in *syn* or *anti* conformation.[36] In monosubstituted π-allyl intermediates (Figure 3a), the *syn* conformation is preferred over the *anti* conformation due to unfavorable $A^{1,3}$ allylic strains in the *anti* manifold.[37] However, the relative population of *anti* π-allyl complex increases in 1,1-disubstituted π-allyl intermediates as both *syn* and *anti* complexes experience destabilizing $A^{1,3}$ allylic strains and 1,2-interactions (Figure 3b). Depending on the steric size of the substituent R^3, either π-allyl intermediate may predominate through equilibration via the $\pi-\sigma-\pi$ mechanism. In order to achieve high enantioselectivity, the catalyst should effectively control the relative populations of *syn* and *anti* complexes because nucleophilic addition onto each π-allyl conformer leads to the formation of the substitution products with opposite stereochemistry.[38] Furthermore, controlling the regioselectivity of nucleophilic addition onto unsymmetrically

https://doi.org/10.1021/jacs.3c04211
J. Am. Chem. Soc. 2023, 145, 19642−19654

Table 1. Examination of Rhodium-Catalyzed Regio- and Enantioselective Substitution of Tertiary Allylic Trichloroacetimidate with Aliphatic Secondary Amine[a,b,c,d]

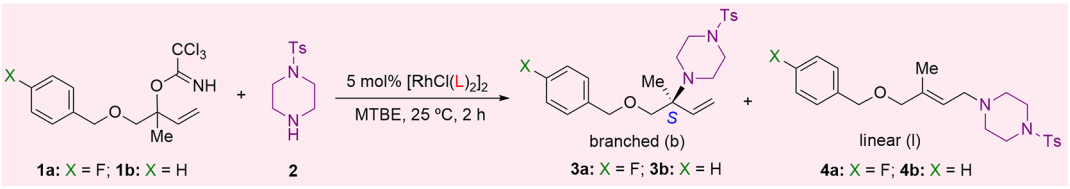

entry	substrate	ligand (L)	yield (%)	ee (%)	b:l ratio
1	(*rac*)-**1a**	NBD	**3a:** 82	0	>99:1
2	(*rac*)-**1a**	(*S*,*S*)-L1	(*S*)-**3a:** 81	95	>99:1
3	(*rac*)-**1b**	(*S*,*S*)-L1	(*S*)-**3b:** 95	94	>99:1
4	(*rac*)-**1b**	(*S*,*S*)-L2	(*S*)-**3b:** 70	90	>99:1
5	(*rac*)-**1b**	(*S*,*S*)-L3	(*S*)-**3b:** 88	98	>99:1
6	(*rac*)-**1b**	(*S*,*S*)-L4	(*S*)-**3b:** 78	40	>99:1
7	(*rac*)-**1b**	(*S*,*S*)-L5	**3b:** 62	0	>99:1
8	(*S*)-**1a** (87% ee)	(*S*,*S*)-L1	(*S*)-**3a:** 93	88	>99:1
9	(*R*)-**1a** (88% ee)	(*S*,*S*)-L1	(*S*)-**3a:** 86	96	>99:1
10	(*rac*)-**1a**	(*R*,*R*)-L1	(*R*)-**3a:** 88	95	>99:1
11	(*R*)-**1a** (88% ee)	NBD	**3a:** 74	3	>99:1

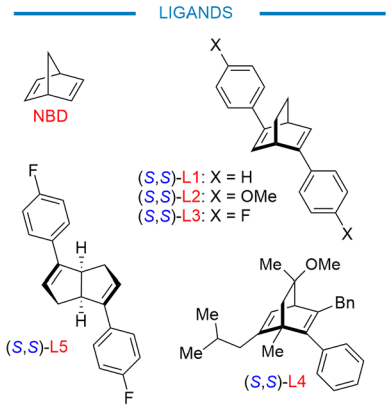

[a]The reaction was carried out using **1a**/**1b** (0.1 mmol), **2** (0.15 mmol), and chiral Rh catalyst (5 mol %) at 25 °C in MTBE for 2 h. [b]Isolated yields. [c]Branched to linear (*b*:l) ratios were determined by ^{1}H NMR of the crude product. [d]The enantiomeric excess (ee) values were determined by HPLC.

substituted π-allylmetal intermediates offers an additional challenge.[39,40] As such, methodologies that could control the branched regioselectivity and/or enantioselectivity of the allylic products have been developed by rationally choosing metals,[41−44] ligands,[45,46] and additive,[47] or by using non-covalent interactions between the allylic electrophile and nucleophilic partner.[48−50]

Despite these major advancements in the transition-metal-catalyzed asymmetric allylic chemistry, methodologies for regio- and enantioselective synthesis of α-tertiary amines featuring tetrasubstituted tertiary carbon remains unreported (Figure 3b). In this context, regio- and enantioselective synthesis of α-trisubstituted α-allylic arylamines has been achieved by our group in 2012[51] and subsequently by others[52,53] employing anilines as nucleophiles. However, amination reactions with secondary aliphatic amines to afford α-trisubstituted-α-tertiary allylic amines have not yet been reported. Aromatic amines are reportedly being utilized as nucleophiles in allylic substitution;[54] use of aliphatic secondary amines as nucleophiles in metal catalysis is less explored due to their ability to coordinate to metal thus inhibiting catalyst turnover and their susceptibility to undergo β-hydride elimination.[55] However, the recent discoveries with the use of secondary aliphatic amines in C−H amination[17,18,23] and allylic substitutions[31−34] illustrate the ability of the metal catalysts to override the Lewis basic nature of aliphatic secondary amines. As a result, we revisited our previously established allylic amination[51] to investigate its feasibility with aliphatic secondary amines. We herein disclose the first example for regio- and enantioselective synthesis of α-trisubstituted-α-tertiary amines based on chiral diene-ligated rhodium-catalyzed asymmetric allylic substitution of racemic tertiary allylic trichloroacetimidates with acyclic and cyclic aliphatic secondary amines (Figure 3c). We also conducted a combined experimental and computational investigation to gain insights into the key aspects of the mechanism. Computations revealed that both *syn* and *anti* π-allyl intermediates are formed upon ionization of racemic allylic substrates; however, *syn* π-allyl manifolds are more reactive than the *anti* forms. Isomerization of π-allyl intermediates via the $\pi-\sigma-\pi$ mechanism is faster than the subsequent outersphere nucleophilic attack, favoring the formation of a single enantiomer of product. The thermodynamically more stable *syn* π-allyl complex was found to be kinetically more reactive, leading to the major (*S*)-branched allylic substituted product. Hydrogen bond interactions between amine-NH and β-oxygen of allylic substrates play a critical role in enabling the high levels of branched selectivity. The chiral diene-ligated rhodium catalyst effectively promotes an asymmetric environment around the *syn* π-allyl moiety, kinetically favoring one diastereomeric allyl complex to undergo nucleophilic substitution, leading to the α-trisubstituted-α-tertiary amine product with high levels of enantioselectivity.

RESULTS AND DISCUSSION

Reaction Development. We first subjected racemic tertiary allylic trichloroacetimidate **1a** and *N*-tosyl piperazine **2** (entry 1, Table 1) to conditions previously developed by our group for rhodium-catalyzed regioselective allylic substitution with anilines.[41] Use of norbornadiene (NBD) rhodium dimer afforded α-trisubstituted-α-tertiary amine **3a** in 82% yield and excellent branched to linear selectivity (*b*:l > 99:1). We then investigated the more challenging enantioselective variant by employing chiral diene-ligated rhodium catalysts that we developed previously for asymmetric synthesis of α-trisubstituted *N*-arylamines.[51] A series of ligands was examined in

https://doi.org/10.1021/jacs.3c04211
J. Am. Chem. Soc. 2023, 145, 19642−19654

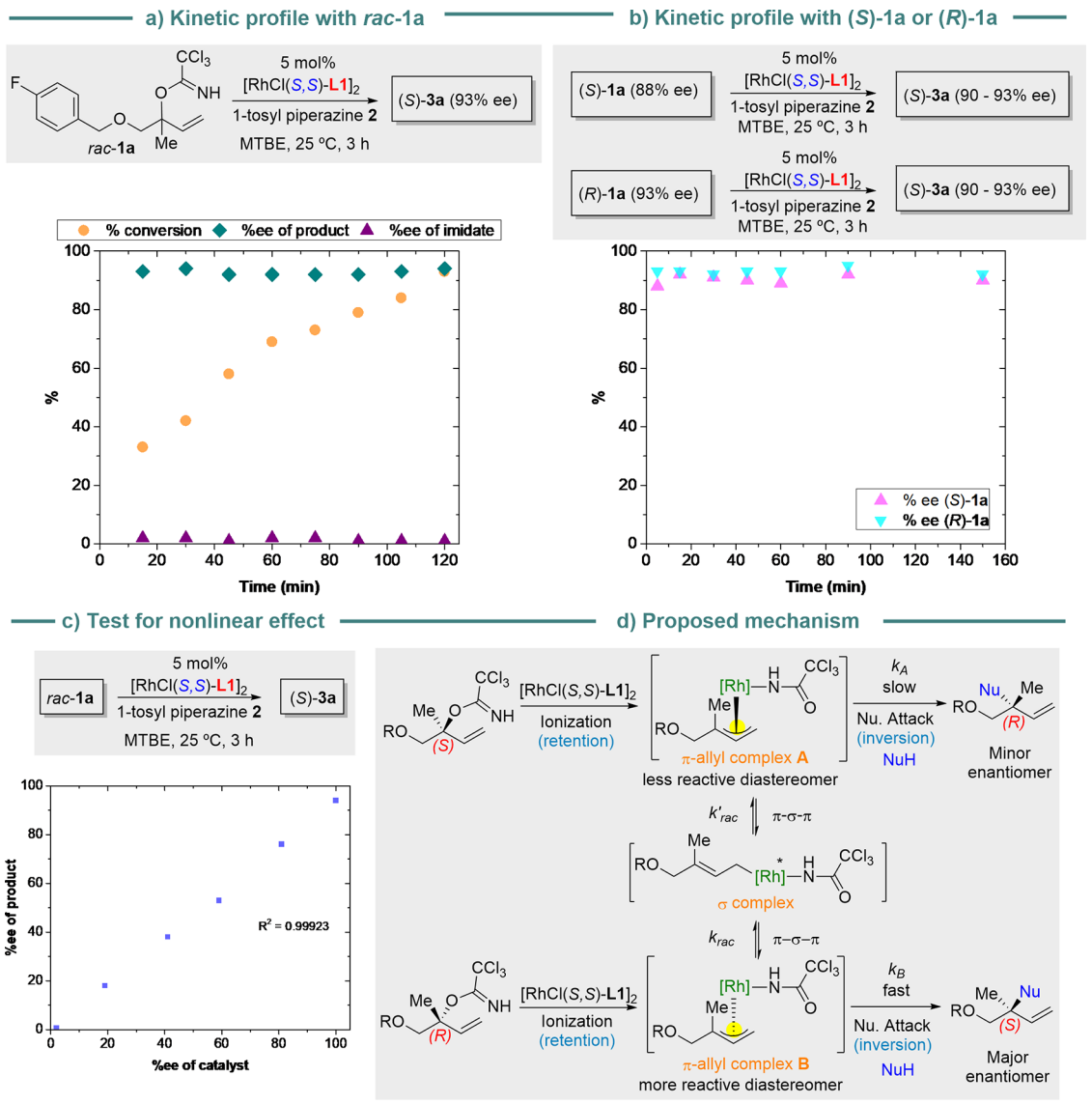

Figure 4. Experimental mechanistic studies (a–c) and (d) proposed the mechanism of Rh-catalyzed asymmetric synthesis of α-trisubstituted-α-tertiary amine.

conjunction with aliphatic secondary amine **2** and (*rac*)-**1a** and (*rac*)-**1b**. Hayashi's diene ligands, **L1**–**L3** (entries 2–5), gave the best match of yield, enantiomeric excess, and branched selectivity. Use of Carreira's ligand **L4** (entry 6)[56] and Lin's ligand **L5** (entry 7)[57] gave a lower asymmetric induction. A ^{13}C NMR study of the ligated diene-rhodium complex was also conducted to rationalize the impact of chiral diene ligands **L1**–**L5** on the observed enantioselectivities (Figure S1 in the SI). In general, the ligated diene ligands exhibit a more upfield shift than the free diene ligands as the hybridization of the metal bound olefinic carbons assume more sp^3 character.[58] The higher coordination shift ($\Delta\delta$) value suggests that the diene binds more strongly to rhodium. Ligands **L1** and **L3** had higher coordination shifts than **L2** (Figure S1 in the SI). These NMR data are consistent with the experimental results that using **L1** and **L3** formed (*S*)-**3b** with higher enantiomeric excess (94–98% ee) than using **L2** (90% ee). Ligand **L4** displayed moderate enantioselectivity (40% ee) because its coordination shift is significantly lower than those of ligands **L1**–**L3**. Use of **L5** resulted in no asymmetric induction presumably due to its poor coordination to rhodium.

Next, we studied reactions of enantioenriched starting materials to elucidate the underlying mechanism. Both (*S*)-**1a** and (*R*)-**1a** substrates were converted into the same product (*S*)-**3a** (Table 1, entries 8 and 9).[39,40] Reaction of (*S*)-**1a** gave a lower enantiomeric excess (88% ee, entry 8) than those obtained from (*rac*)-**1a** (95% ee, entry 2) and (*R*)-**1a** (96% ee, entry 9). On the other hand, reaction of (*rac*)-**1a** with amine **2** mediated by [RhCl(*R*,*R*)-**L1**]$_2$ afforded (*R*)-**3a** product (entry 10) with opposite stereochemistry to that with [RhCl(*S*,*S*)-**L1**]$_2$ (entry 2). We also conducted reaction of (*R*)-**1a** with **2** using an achiral NBD ligand (entry 11), which has a similar backbone structure to chiral diene ligand **L1**. This reaction proceeded to afford product **3a** almost as a racemate. This result suggests that the enantiomeric π-allyl complex intermediates derived from ionization of (*R*)-**1a** interconvert faster than the subsequent amine attack, thereby resulting racemic products and supporting a potential dynamic kinetic asymmetric transformation (DYKAT) mechanism.[39,40,59]

https://doi.org/10.1021/jacs.3c04211
J. Am. Chem. Soc. 2023, 145, 19642–19654

Mechanism. To validate that the α-amination reaction does not proceed through a kinetic resolution of the racemic mixture, enantiomeric excess of (*S*)-**3a** product and (*rac*)-**1a** starting material were measured by HPLC equipped with chiral columns while monitoring reaction progress with ^{19}F NMR. As illustrated in Figure 4a, enantiomeric excess of (*S*)-**3a** remained high (>90% ee) during the progress of the reaction. In addition, starting material **1a** remained racemic throughout the course of the reaction, indicating similar rates of consumption for both enantiomers of *rac*-**1a**. The results obtained in Figure 4a invalidates a potential kinetic resolution. Further independent experiments with both starting materials (*S*)-**1a** and (*R*)-**1a** indicated that they did not racemize as their enantiomeric excess values remained unchanged (Figure 4b). This result attests that the reaction does not undergo dynamic kinetic resolution (DKR); in such case, a significant depletion in the enantiomeric excess of the starting material would be expected due to racemization.[60,61]

To gain insight into the coordination mode of the chiral ligand during the catalytic reaction, we tested the dependence of enantioselectivity of the reaction with the enantiopurity of the ligand (Figure 4c). Such experiments provide important information on the composition of the Rh catalyst species in the reaction mixture as nonlinear effects typically interpret the presence of one or more species that contain multiple units of chiral entity.[62] A linear relationship was observed between the enantiomeric excess of the rhodium catalyst and (*S*)-**3a** product (Figure 4c), indicating that the active catalyst species in the enantio-discriminating step most likely has one chiral diene ligand coordinated to the Rh center.[63,64]

Based on the data obtained in Figure 4a–c, a proposed mechanism using [RhCl(*S*,*S*)-**L1**]$_2$ is shown in Figure 4d. Our group has previously reported that trichloroacetimidate serves as a leaving group and directing group to facilitate ionization of allylic substrate to form π-allyl complexes with retention of stereochemistry.[65] As a result, we proposed that both (*S*)- and (*R*)-enantiomers of starting material would ionize to form diastereomeric π-allyl intermediate **A** and **B**, respectively. Nucleophilic attack with inversion onto π-allyl complex **B** would afford the major (*S*)-product. On the other hand, π-allyl complex **A** would first undergo $\pi-\sigma-\pi$ interconversion to transform into the more reactive π-allyl complex **B**, leading to the (*S*)-product. To attain high levels of enantioselectivity, two diastereomeric π-allyl complexes should rapidly interconvert via the $\pi-\sigma-\pi$ mechanism, and one π-allyl complex should react significantly faster with secondary amine than its diastereomer, therefore establishing Curtin Hammett conditions ($k_{rac} \gg k_B \gg k_A$).

As shown in Figure 4d, we assume that an outersphere nucleophilic attack is operative in the C–N bond formation.[66] However, an innersphere attack by aliphatic amine onto the π-allyl intermediate cannot be excluded. Thus, we conducted experiments using deuterium-labeled enantiomeric forms of starting material **1c** to establish the nature of nucleophilic addition. Both deuterium labeled (*S*)-**1c** and (*R*)-**1c** were submitted to the reactions with amine **2** using [RhCl(*S*, *S*)-**L1**]$_2$ as the catalyst (Figure 5). The reaction of deuterium-labeled (*S*)-**1c** afforded (*S*)-**3c** with transposition of the deuterium atom at the terminal olefinic carbon from 83% *Z* to 82% *E* (Figure 5A). In contrast, the amination reaction of deuterium-labeled (*R*)-**1c** occurred with retention of (*Z*) olefin geometry (91% *Z* → 90% *Z*) (Figure 5B). These data are consistent with a retention-π-σ-π racemization-inversion pathway for the (*S*)-allylic starting material (Figure 4d), while a retention-inversion pathway for the (*R*)-allylic starting material. Taken together, the data support that nucleophilic attack onto π-allyl intermediate occurs via an *outersphere* mechanism.

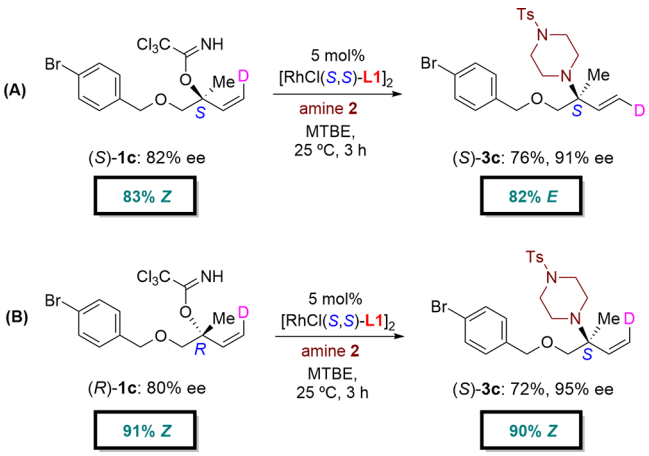

Figure 5. Substitution of enantioenriched deuterium-labeled trichloroacetimidate substrates.

To provide insight into the selectivity of the α-amination reaction, density functional theory (DFT) calculations were employed to examine the coordination complexes as well as the key transition states and intermediates. We previously reported the ability of the chiral diene-ligated rhodium catalyst to promote asymmetric α-amination of racemic tertiary allylic trichloroacetimidates with a variety of anilines as a direct and efficient route to access α-trisubstituted-α-allylic arylamines.[51] As such, β-methoxy substrate **5** and aniline **6** were chosen as model substrates for all calculations to reduce the computational cost. To validate the feasibility of these substrates, the reaction of **5** and **6** was performed under optimized conditions to provide α-trisubstituted amine **7** (Scheme 1a) in good yield and selectivity (85%, 92% ee, *b*:l > 99:1).

To further support that the reaction of anilines is likely to proceed through dynamic kinetic asymmetric transformation similar to that of secondary aliphatic amines (Figure 4a,b), two additional kinetic profiles were conducted by employing **1a** as the electrophilic partner in the reaction with aniline **6**. As demonstrated in Scheme 1a, the reaction of (*rac*)-**1a** with aniline **6** afforded α-trisubstituted-α-allylic arylamine product **6a** in 83% yield and 88% ee. Next, we monitored this reaction by HPLC equipped with chiral columns, and the result revealed that allylic substrate **1a** remained racemic during the course of the amination reaction (Scheme 1b). Likewise, when the enantioenriched starting material, (*R*)-**1a**, was used in the reaction, the enantiopurity of (*R*)-**1a** was retained throughout the reaction (Scheme 1c). This result, in combination with the data obtained in Figure 4b, suggests that the ionization step (see Figure 4d) is not reversible. Overall, these data obtained with aniline **6** are on par with those observed with aliphatic secondary amine **2** (Table 1 and Figure 4a,b). Collectively, these findings provide additional support for utilizing aniline in the calculations as reactions with both aniline and aliphatic secondary amines are likely to proceed via the dynamic kinetic asymmetric transformation (DYKAT) pathway.

The experimental evidence in Figure 4c suggested a monomeric rhodium complex as the active catalyst in the enantio-discriminating step. Computational studies were then employed to investigate the possible modes of coordination of

https://doi.org/10.1021/jacs.3c04211
J. Am. Chem. Soc. 2023, 145, 19642–19654

Scheme 1. Investigation of Reactions of Allylic Substrates 5 and 1a with Aniline 6

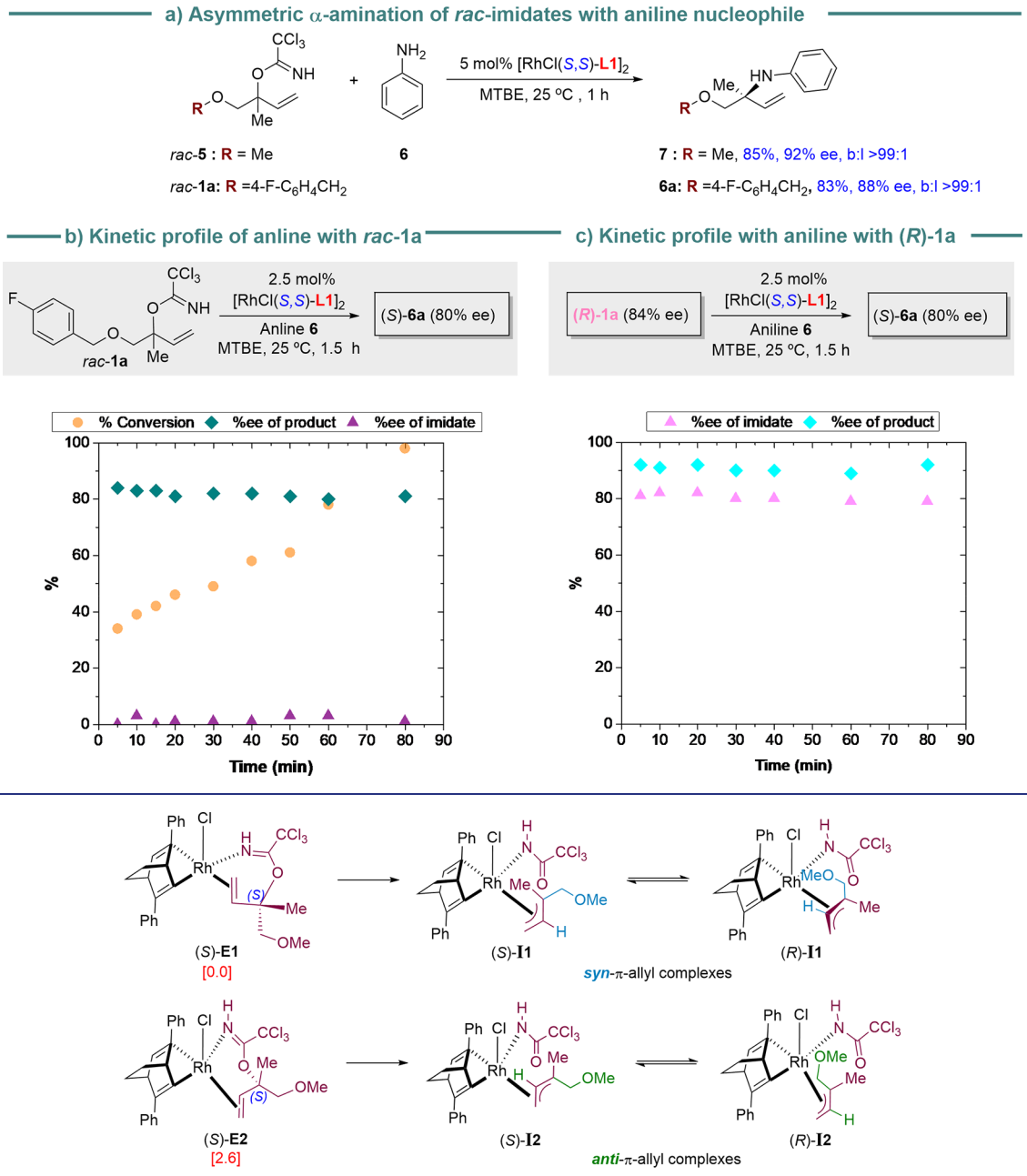

Figure 6. Possible modes of rhodium coordination to allylic trichloroacetimidate and formation of π-allyl complexes.

monomeric RhCl(*S*,*S*)-**L1** complex to (*S*)- and (*R*)-allylic substrate **5** (Figure 6). After extensive conformational analysis, five distinct isomeric structures were identified for coordination of the rhodium catalyst to both (*S*)- and (*R*)-**5** (see Figures S3 and S4 in the SI). Calculations revealed a strong energetic preference for bidentate coordination of **5**, via η^2-(π-coordination) of the olefin and η^1-(σ-coordination) to the trichloroacetimidate nitrogen, forming a pentacoordinated square pyramidal complex such as (*S*)-**E1** and (*S*)-**E2** (Figure 6). We identified 16 diastereomeric π-allyl rhodium complexes arising from ionization of (*S*)- and (*R*)-substrate **5** (see Scheme S3 as well as Figures S2 and S7 in the SI). Our calculations also indicated that the (*S*)-*syn* and (*R*)-*syn* π-allylrhodium complexes can undergo interconversion via a σ-complex. Similarly, the (*S*)-*anti* and (*R*)-*anti* complexes could also interconvert (Figure 6 and Scheme S3 in the SI). However, conversion of a *syn* complex to the corresponding *anti* complex is not feasible and vice versa.

We also computed the activation free energies leading to the branched product **7** from each π-allyl complex (Figure 7 as well as Figures S2 and S9 in the SI). Although both *syn* and *anti* π-allyl rhodium intermediates lead to (*S*)-**7** as the major product, the *anti* π-allyl pathway (Figure S2 in the SI) proceeds through a higher energy than the competing *syn* π-allyl pathway. For simplicity, we focus on the energetically more favorable pathway that involves *syn* π-allyl intermediates (*S*)-**I1** and (*R*)-**I1** derived from complexes (*S*)-**E1** and (*R*)-**E1**, respectively (Figure 7). From the (*S*)-**5** starting material, the C−O bond cleavage via transition state (*S*)-**TS1** (relative energy barrier is 13.4 kcal/mol from (*S*)-**E1**) leads to the *syn* π-

https://doi.org/10.1021/jacs.3c04211
J. Am. Chem. Soc. 2023, 145, 19642−19654

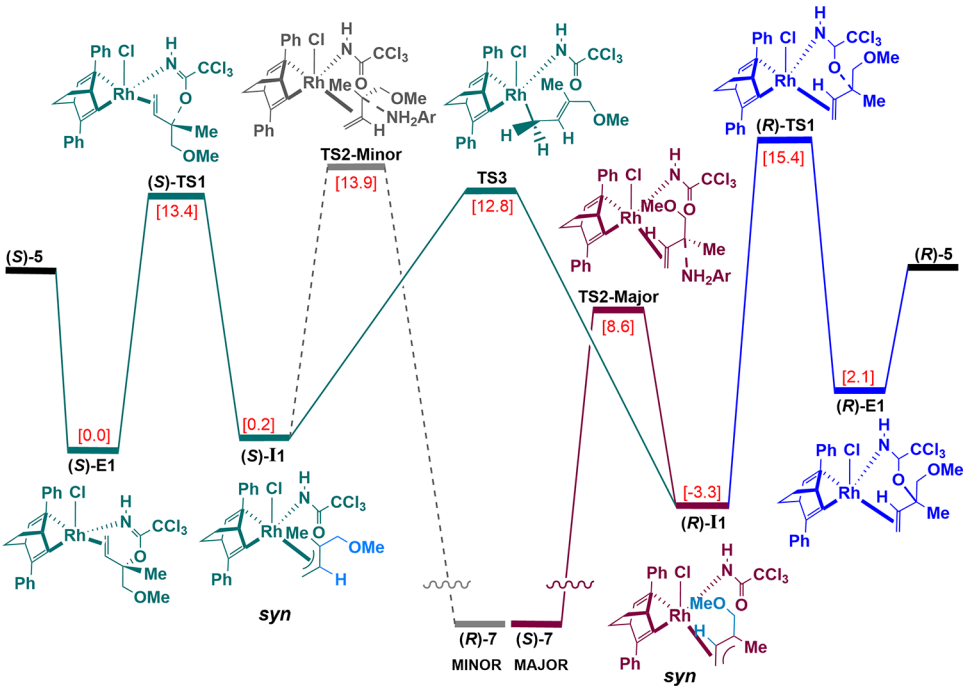

Figure 7. Energy profile for the asymmetric synthesis of α-trisubstituted-α-allylic amine. Free energies (kcal/mol) were computed using PBE1PBE/6-311+G(d,p) (diethyl ether).

allyl intermediate, (*S*)-**I1**, downhill in energy by 13.2 kcal/mol. We discovered two competing pathways stemming from the π-allyl intermediate (*S*)-**I1** that include the nucleophilic addition transition state **TS2-Minor** and π-allyl isomerization transition state **TS3**. The barrier for aniline attack onto the *syn* π-allyl intermediate (*S*)-**I1**, via **TS2-Minor**, leading to minor branched amine (*R*)-**7**, is higher in energy (13.9 kcal/mol) than the barrier for isomerization (12.8 kcal/mol) of the *syn* π-allyl intermediate (*S*)-**I1** to *syn* π-allyl (*R*)-**I1** via **TS3**, which eventually leads to the major product (*S*)-**7**. In contrast, the *syn* π-allyl intermediate (*R*)-**I1**, generated from ionization of (*R*)-**5** starting material via transition state (*R*)-**TS1** (barrier of 15.4 kcal/mol), favors direct nucleophilic attack by aniline **6** to give the major product (*S*)-**7** via transition state **TS2-Major** with a barrier of 8.6 kcal/mol. The facile isomerization of (*S*)-**I1** to its diastereomer (*R*)-**I1** is the key process that enables the conversion of the racemic starting material into a single enantiomer of the product through the DYKAT mechanism.

Our calculations show that (*R*)-**I1** derived from ionization of (*R*)-**5** is the more reactive and stable intermediate than (*S*)-**I1** (Figure 7). Computations also showed that (*R*)-**I1** is stabilized by developing lone pair-π interactions[67] between oxygen of the π-allyl moiety and the phenyl rings of the diene ligand (see Figure S7 in the SI). On the other hand, steric repulsions between the methoxy group of the π-allyl moiety and the trichloroacetamide group bound to the rhodium center destabilize the (*S*)-**I1** intermediate. This computational result was further supported by deuterium-labeling experiments (Figure 5), wherein (*R*)-**1c** proceeded with the retention of the *Z*-olefin geometry, confirming that (*S*)- and (*R*) enantiomers of allylic substrate converged to the amine product via the major π-allyl intermediate derived from the (*R*)-isomer. This further clarifies why (*R*)-**1a** formed **3a** with higher selectivity than the reaction with (*S*)-**1a** (Table 1, entry 9 vs entry 8).

Next, we sought to investigate the factors contributing to high branched selectivity. For simplicity, we only discuss addition of aniline **6** onto complexes (*S*)-**I1** and (*R*)-**I1**, leading to the branched and linear products (Figure 8). The computed barrier of transition states **TS2-Linear** and **TS2′-Linear** for aniline attack onto the *syn* π-allyl intermediates (*R*)-**I1** (18.0 kcal/mol, Figure 8A) and (*S*)-**I1** (22.1 kcal/mol, Figure 8B) leading to the linear product was significantly higher in energy than those barriers of transition states **TS2-Minor** (13.9 kcal/mol) and **TS2-Major** (8.6 kcal/mol) leading to the branched (*R*)-**7** and (*S*)-**7**, respectively. A closer inspection of **TS2-Minor** and **TS2-Major** reveals that the aniline NH involves in a hydrogen bond interaction with the β-oxygen of the substrate (O−H−N = 2.16 Å), forming a five-membered transition state whereas such a hydrogen bond interaction was not observed in **TS2-Linear** transition states. Unfavorable interactions were also observed in **TS2-Linear** transition states between (a) the β-methoxy of the π-allyl moiety and the ligand's phenyl ring (Figure 8A); (b) the α-methyl of the π-allyl moiety and the ligand's phenyl ring (Figure 8B); and (c) the β-methoxy of the π-allyl moiety and the phenyl ring of aniline (Figure 8B).

Regarding the enantioselectivity, the barrier for aniline attack onto the *syn* π-allyl rhodium intermediate (*S*)-**I1** (13.9 kcal/mol, Figure 8B) leading to the minor product (*R*)-**7** is significantly higher in energy than that onto the *syn* π-allyl rhodium intermediate (*R*)-**I1** (8.6 kcal/mol, Figure 8A) leading to the major product (*S*)-**7**. Inspection at **TS2-Minor** and **TS2-Major** transition states revealed that the α-CH_3 group of the π-allyl moiety had an unfavorable interaction with the ligand's phenyl ring and aniline in **TS2-Minor,** leading to (*R*)-**7** while the α-CH_3 group pointed away from the phenyl rings in **TS2-Major**, leading to the major (*S*)-**7** product.

Substrate Scope. After we established the mechanism of α-amination, we examined the scope of 12 cyclic secondary amines frequently encountered in aliphatic α-tertiary amine

https://doi.org/10.1021/jacs.3c04211
J. Am. Chem. Soc. 2023, 145, 19642−19654

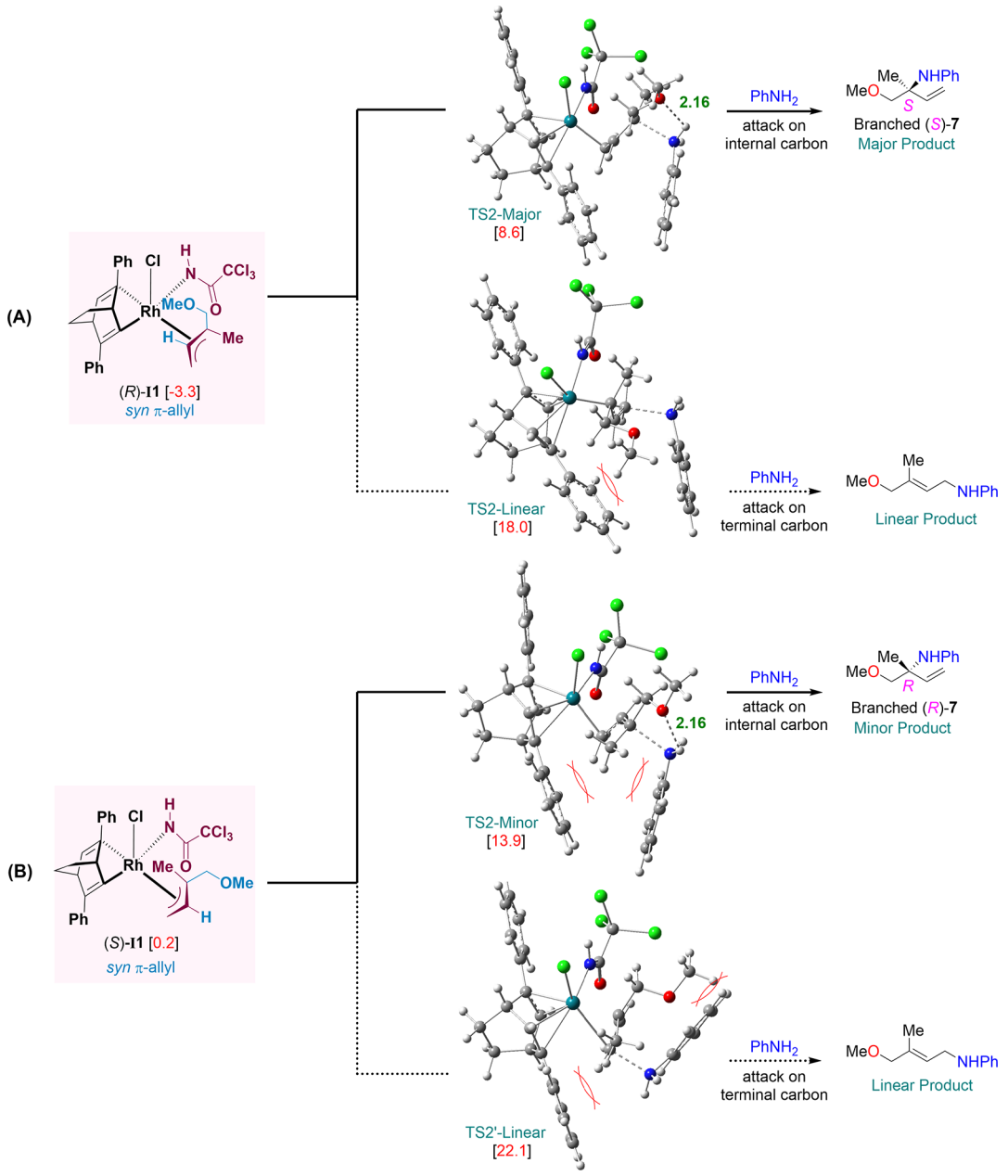

Figure 8. (A) Transition state for major branched (*S*)-**7** and linear product. (B) Transition state for minor branched (*R*)-**7** and linear product.

pharmaceuticals (Table 2).[2,4] Reactions of these cyclic amines with racemic starting materials containing *β*-oxygen afforded the substitution products **8**−**19** and **21** in 65−99% yield and 76−99% ee. We also investigated if enantioenriched (*R*)-2-methyl indoline could influence the diastereoselectivity of the *α*-trisubstituted-*α*-tertiary amine product using both (*S*,*S*)-**L1** and (*R*,*R*)-**L1** ligands. Amine-rhodium catalyst matching and mismatching effect was observed in the reaction with (*rac*)-allylic substrate **1b**. In the mismatched case, use of (*S*,*S*)-**L1** provided **21** with moderate diastereocontrol (*dr* = 6:1). In the matched case, use of (*R*,*R*)-**L1** provided **21** with excellent diastereoselectivity (*dr* = 1:19). Acyclic secondary *N*-methylpropargylamine and *N*-methylbenzylamine, that are more prone to undergo *β*-hydride elimination than their cyclic amine counterparts,[55] also effectively underwent *α*-amination to deliver **22**−**24** in 74−95% yield and excellent enantioselectivity (90−95% ee). We discovered that the sterically hindered *N*-propylphenylamine was also highly efficient, affording *α*-trisubstituted-*α*-tertiary amine **25** in 81% yield and 86% ee.

Due to the privileged nature of 1,2-diamines, efforts have been focused on developing catalytic asymmetric methodologies for their construction.[68−71] To date, construction of chiral 1,2-diamines bearing *α*-trisubstituted-*α*-tertiary amine motifs remains underdeveloped.[72] Although tertiary allylic substrates bearing *β*-nitrogen-containing heterocycles could undergo *α*-amination reaction to generate 1,2-diamines, competing formation of vinyl aziridine intermediate could erode the enantioselectivity of the substitution products due to the presence of the *β*-nitrogen atom proximal to the electrophilic site of the reactive *syn π*-allyl complex.[73] This shortcoming could be addressed through the judicious choice of functional groups that could decrease nitrogen nucleophilicity and consequently suppressing vinyl aziridine formation.

https://doi.org/10.1021/jacs.3c04211
J. Am. Chem. Soc. 2023, 145, 19642−19654

Table 2. Substrate Scope of Aliphatic Secondary Amines and Tertiary Allylic Electrophiles[a]

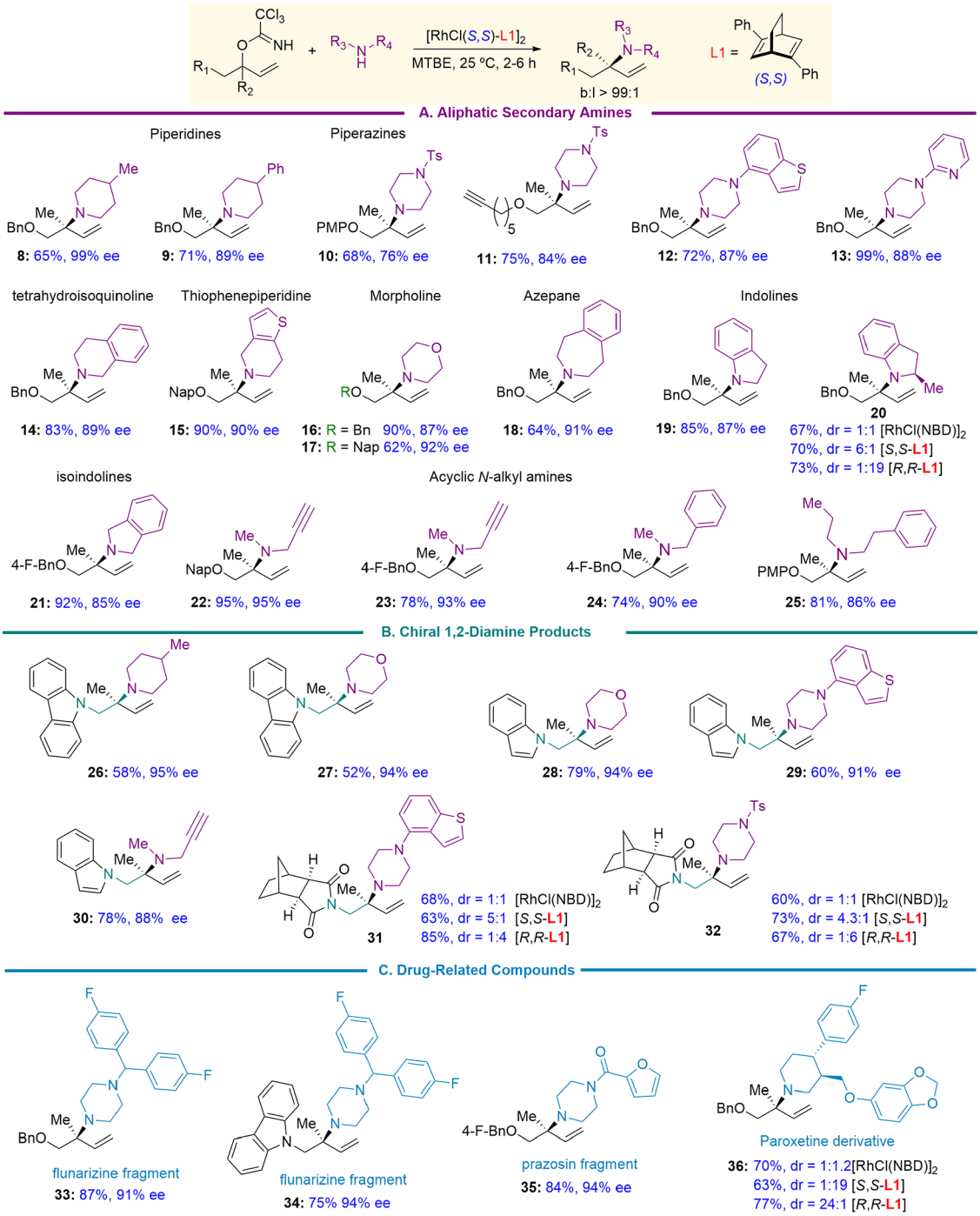

[a]Reaction conditions: amine (0.15 mmol), trichloroacetimidate (0.1 mmol), 5 mol % [RhCl(*S*,*S*)-**L1**) in MTBE (1 mL) under nitrogen atmosphere at 25 °C for 2 h. MTBE, methyl *tert*-butyl ether.

Since the nitrogen lone pairs of carbazole and indole participate in the π-system of the aromatic ring, we hypothesized that they would not be available to promote vinyl aziridine formation. Accordingly, reaction with carbazole and indole-containing allylic substrates provided **26**−**30** in synthetically useful yield (52−79%) and excellent enantioselectivity (88−95% ee).

Encouraged by the results obtained for the enantioenriched 1,2-diamines products **26**−**30** (Table 2), we next explored the reaction with β-norbornanedicarboximide-substituted substrate to study the allylic substrate-catalyst matching and mismatching effect due to the presence of the pre-existing stereocenters on the substrate. As demonstrated in Table 2, use of (*S*,*S*)-**L1** ligand provided 1,2-diamine products **31** and **32** with moderate diastereocontrol (*dr* = 5:1 and 4.3:1). Use of (*R*,*R*)-**L1** also furnished **31** and **32** with similar diastereoselectivity (*dr* = 1:4 and 1:6). These results suggest that the chiral rhodium catalyst partially overrides substrate inherent bias.

https://doi.org/10.1021/jacs.3c04211
J. Am. Chem. Soc. 2023, 145, 19642−19654

Finally, access to enantioenriched α-trisubstituted-α-tertiary amines by rhodium-catalyzed asymmetric amination provides an opportunity for the expedient synthesis of a number of drug analogs. These pharmaceutical derivatives **33**−**35** were readily synthesized from α-amination of cyclic and acyclic secondary amines in good yield and excellent levels of enantioselectivity. Despite the distinct stereochemical properties and complex structure, paroxetine underwent highly diastereoselective α-amination to afford **36** using either (*S*,*S*)-**L1** ligand (*dr* = 1:19) or (*R*,*R*)-**L1** (*dr* = 24:1). These substitution amine products are amendable for further functionalization in drug discovery screening.[74]

In addition to β-oxygen and nitrogen-substituted allylic substrates, we attempted amination of γ-oxygen substituted allylic trichloroacetimidate **37a** with aliphatic amine **2** and aniline **6** to test the limitation of our methodology. The substitution products **37** and **38** (Scheme 2) were obtained in good yields (67 and 82%) and moderate levels of enantioselectivity (51% ee and 57% ee). However, the reaction underwent highly branched selectivity (*b*:l > 99:1) as evident by strong hydrogen bonding interactions between aniline-NH and γ-oxygen of the allylic substrate (O−H−N = 1.87 Å) forming six-membered transition states (Figure 9). Interestingly, hydrogen bonding interactions between aniline-NH and γ-oxygen are stronger than those between aliphatic secondary amine-NH and β-oxygen (O−H−N = 2.16 Å, Figure 8).

Scheme 2. Rhodium-Catalyzed Asymmetric Amination with γ-Oxygen-Substituted Tertiary Allylic Trichloroacetimidate

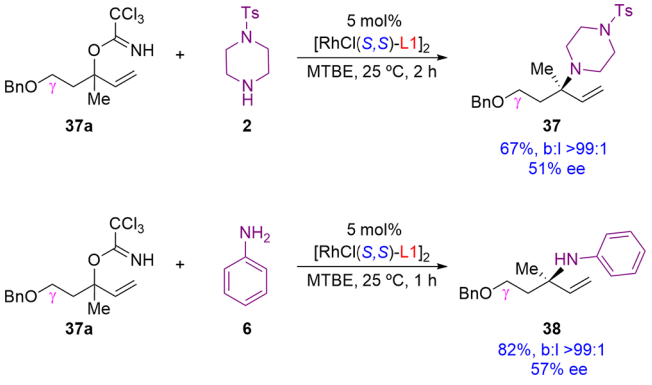

To understand factors causing the erosion of enantioselectivity, DFT calculations were also carried out using γ-methoxy substituted tertiary allylic trichloroacetimidate as a model substrate (Figure 9). Interestingly, ionization of (*S*)-substrate favors formation of *anti* π-allyl species, (*S*)-**I3** whereas (*R*)-enantiomer favors formation of *syn* π-allyl species, (*R*)-**I3**. This is in contrast to what had been observed with β-oxygen allylic substrates, wherein both enantiomers of substrate underwent reaction via the *syn* π-allyl pathway. The transition state barriers for nucleophilic attack of aniline onto the (*S*)-**I3** and (*R*)-**I3** leading to formation of (*R*)- and (*S*)-γ-oxygen substituted products are similar in energy (8.0 and 6.9 kcal/mol, respectively, Figure 9), which is consistent with our experimental results (57% ee, Scheme 2). To compare, the transition state barriers leading to the formation of (*R*)- and (*S*)-β-oxygen substituted products are significantly different in energy (13.9 and 8.6 kcal/mol, respectively, Figure 8). Overall, these computational data explain why amination of β-oxygen substrates afforded α-trisubstituted-α-tertiary amine products with excellent enantioselectivity (Table 2) while reaction of γ-oxygen substrates only resulted in moderate levels of asymmetric induction.

CONCLUSIONS

In summary, we report an efficient strategy for the enantioselective construction of α-trisubstituted-α-tertiary amines by rhodium-catalyzed asymmetric allylic substitutions of racemic tertiary allylic trichloroacetimidates. The substitutions occur with a variety of acyclic and cyclic secondary amines to afford α-trisubstituted-α-tertiary amine products with complete conversion, excellent branched selectivity, and high enantioselectivity. Mechanistic studies using combined experimental and computational data support that the α-amination reaction of racemic tertiary allylic substrates with

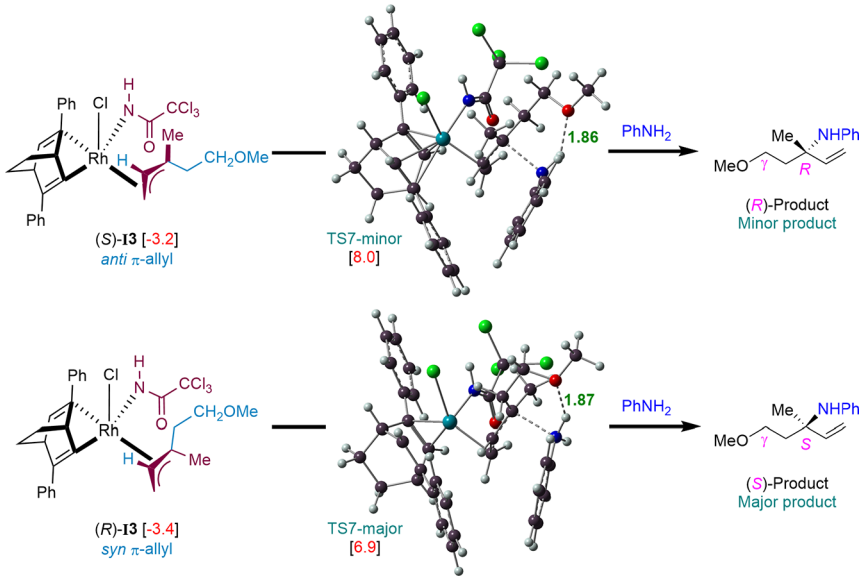

Figure 9. Relative energies of amine addition to the γ-oxygen-substituted substrate. Free energies (kcal/mol) were computed using PBE1PBE/6-311+G(d,p) (diethyl ether).

https://doi.org/10.1021/jacs.3c04211
J. Am. Chem. Soc. 2023, 145, 19642−19654

aliphatic secondary amines is likely to occur via a DYKAT process. Furthermore, DFT calculations and deuterium-labeled trichloroacetimidate experiments validate that enantioselective C−N bond formation proceeds via an *outersphere* mechanism at the more substituted carbon of the allyl moiety. In addition, computational data demonstrate that in contrast to the monosubstituted secondary allylic substrate wherein *syn* π-allyl complexes are the reactive intermediates, both *syn* and *anti* π-allyl rhodium intermediates lead to the major product in 1,1-disubstittued tertiary allylic substrates. The *anti* π-allyl pathway proceeds through a higher energy transition state than the competing *syn* π-allyl pathway. Our calculations also show that interconversion of the *syn* complex to its *anti* form is not feasible and vice versa; however, (*S*)-*syn* and (*R*)-*syn* π-allyl complexes can interconvert via σ-complex; likewise, (*S*)-*anti* and (*R*)-*anti* can also interconvert. Hydrogen bond interactions between amine-NH and β-oxygen of allylic substrates are critical for the observed branched selectivity. Although the present reaction is effective on substrates bearing β-oxygen and nitrogen substituents, we anticipate that our study provides a foundation for the development of transition-metal catalyzed asymmetric allylic substitution reactions to afford a broad range of enantioenriched α-trisubstituted-α-tertiary amines.

■ ASSOCIATED CONTENT

Supporting Information

The Supporting Information is available free of charge at https://pubs.acs.org/doi/10.1021/jacs.3c04211.

General synthesis of the key intermediates; tertiary allylic trichloroacetimidates; α-trisubstituted-α-tertiary amine products; and HPLC traces of α-trisubstituted-α-tertiary amine products, as well as ^{1}H, ^{13}C, and ^{19}F NMR spectra of synthetic compounds (PDF)

■ AUTHOR INFORMATION

Corresponding Authors

H. Bernhard Schlegel − *Department of Chemistry, Wayne State University, Detroit, Michigan 48202, United States;* orcid.org/0000-0001-7114-2821; Email: hbs@chem.wayne.edu

Hien M. Nguyen − *Department of Chemistry, Wayne State University, Detroit, Michigan 48202, United States;* orcid.org/0000-0002-7626-8439; Email: hmnguyen@wayne.edu

Authors

Madhawee K. Arachchi − *Department of Chemistry, Wayne State University, Detroit, Michigan 48202, United States*

Richard N. Schaugaard − *Department of Chemistry, Wayne State University, Detroit, Michigan 48202, United States*

Complete contact information is available at: https://pubs.acs.org/10.1021/jacs.3c04211

Author Contributions

The project was conceived of and supervised by H.M.N while M.K.A. developed the rhodium-catalyzed asymmetric synthesis of α-trisubstituted-α-tertiary amines and performed the reaction mechanistic studies. H.B.S. and R.N.S. performed DFT studies. H.M.N. and M.K.A. wrote the manuscript and incorporated revisions suggested by H.B.S.

Notes

The authors declare no competing financial interest.

■ ACKNOWLEDGMENTS

Financial support from Carl Johnson Endowed Chair and NIGMS (R35GM149213) for H.M.N and NSF (CHE1856437) for H.B.S. is acknowledged. M.K.A. thanks Wayne State University for the Rumble graduate fellowship. The Wayne State University Lumigen Center was partially supported by NIH (S10OD028488 for NMR and R01GM098285 for Mass Spect). We also thank the Wayne State University Grid for computing resources.

■ REFERENCES

(1) Hager, A.; Vrielink, N.; Hager, D.; Lefranc, J.; Trauner, D. Synthetic approaches towards alkaloids bearing alpha-tertiary amines. *Nat. Prod. Rep.* **2016**, *33*, 491−522.

(2) Vitaku, E.; Smith, D. T.; Njardarson, J. T. Analysis of the Structural Diversity, Substitution Patterns, and Frequency of Nitrogen Heterocycles among U.S. FDA Approved Pharmaceuticals. *J. Med. Chem.* **2014**, *57*, 10257−10274.

(3) Trowbridge, A.; Walton, S. M.; Gaunt, M. J. New Strategies for the Transition-Metal Catalyzed Synthesis of Aliphatic Amines. *Chem. Rev.* **2020**, *120*, 2613−2692.

(4) Roughley, S. D.; Jordan, A. M. The Medicinal Chemist's Toolbox: An Analysis of Reactions Used in the Pursuit of Drug Candidates. *J. Med. Chem.* **2011**, *54*, 3451−3479.

(5) Morgenthaler, M. Predicting and Tuning Physicochemical Properties in Lead Optimization: Amine Basicities. *ChemMedChem* **2007**, *2*, 1100−1115.

(6) Cabre, A.; Verdaguer, X.; Riera, A. Recent Advances in the Enantioselective Synthesis of Chiral Amines via Transition Metal-Catalyzed Asymmetric Hydrogenation. *Chem. Rev.* **2022**, *122*, 269−339.

(7) Yin, Q.; Shi, Y. J.; Wang, J. X.; Zhang, X. M. Direct catalytic asymmetric synthesis of alpha-chiral primary amines. *Chem. Soc. Rev.* **2020**, *49*, 6141−6153.

(8) Cogan, D. A.; Ellman, J. A. Asymmetric Synthesis of α,α-Dibranched Amines by the Trimethylaluminum-Mediated 1,2-Addition of Organolithiums to tert-Butanesulfinyl Ketimines. *J. Am. Chem. Soc.* **1999**, *121*, 268−269.

(9) Shintani, R.; Takeda, M.; Tsuji, T.; Hayashi, T. Rhodium-Catalyzed Asymmetric Arylation of N-Tosyl Ketimines. *J. Am. Chem. Soc.* **2010**, *132*, 13168−13169.

(10) Yang, Y.; Shi, S. L.; Niu, D. W.; Liu, P.; Buchwald, S. L. Catalytic asymmetric hydroamination of unactivated internal olefins to aliphatic amines. *Science* **2015**, *349*, 62−66.

(11) Adamson, N. J.; Hull, E.; Malcolmson, S. J. Enantioselective Intermolecular Addition of Aliphatic Amines to Acyclic Dienes with a Pd-PHOX Catalyst. *J. Am. Chem. Soc.* **2017**, *139*, 7180−7183.

(12) Yang, X. H.; Dong, V. M. Rhodium-Catalyzed Hydrofunctionalization: Enantioselective Coupling of Indolines and 1,3-Dienes. *J. Am. Chem. Soc.* **2017**, *139*, 1774−1777.

(13) Long, J.; Wang, P.; Wang, W.; Li, Y. Q.; Yin, G. Y. Nickel/Bronsted Acid-Catalyzed Chemo- and Enantioselective Intermolecular Hydroamination of Conjugated Dienes. *iScience* **2019**, *22*, 369.

(14) Vanable, E. P.; Kennemur, J. L.; Joyce, L. A.; Ruck, R. T.; Schultz, D. M.; Hull, K. L. Rhodium-Catalyzed Asymmetric Hydroamination of Allyl Amines. *J. Am. Chem. Soc.* **2019**, *141*, 739−742.

(15) Kawatsura, M.; Hartwig, J. F. Palladium-catalyzed intermolecular hydroamination of vinylarenes using arylamines. *J. Am. Chem. Soc.* **2000**, *122*, 9546−9547.

(16) Adamson, N. J.; Malcolmson, S. J. Catalytic Enantio- and Regioselective Addition of Nucleophiles in the Intermolecular Hydrofunctionalization of 1,3-Dienes. *ACS Catal.* **2020**, *10*, 1060−1076.

(17) Ali, S. Z.; Budaitis, B. G.; Fontaine, D. F. A.; Pace, A. L.; Garwin, J. A.; White, M. C. Allylic C-H amination cross-coupling

furnishes tertiary amines by electrophilic metal catalysis. *Science* **2022**, *376*, 276−283.
(18) Jin, Y.; Jing, Y.; Li, C.; Li, M.; Wu, W.; Ke, Z.; Jiang, H. Palladium-catalysed selective oxidative amination of olefins with Lewis basic amines. *Nat. Chem.* **2022**, *14*, 1118−1125.
(19) Clayden, J.; Donnard, M.; Lefranc, J.; Tetlow, D. J. Quaternary centres bearing nitrogen (α-tertiary amines) as products of molecular rearrangements. *Chem. Commun.* **2011**, *47*, 4624−4639.
(20) Goswami, P.; Cho, S. Y.; Park, J. H.; Kim, W. H.; Kim, H. J.; Shin, M. H.; Bae, H. Y. Efficient access to general alpha-tertiary amines via water-accelerated organocatalytic multicomponent allylation. *Nat. Commun.* **2022**, *13*, 2702.
(21) Henry Blackwell, J.; Harris, G. R.; Smith, M. A.; Gaunt, M. J. Modular Photocatalytic Synthesis of α-Trialkyl-α-Tertiary Amines. *J. Am. Chem. Soc.* **2021**, *143*, 15946−15959.
(22) Gao, X.; Turek-Herman, J. R.; Choi, Y. J.; Cohen, R. D.; Hyster, T. K. Photoenzymatic Synthesis of α-Tertiary Amines by Engineered Flavin-Dependent "Ene"-Reductases. *J. Am. Chem. Soc.* **2021**, *143*, 19643−19647.
(23) Pak Shing Cheung, K.; Fang, J.; Mukherjee, K.; Mihranyan, A.; Gevorgyan, V. Asymmetric intermolecular allylic C-H amination of alkenes with aliphatic amines. *Science* **2022**, *378*, 1207−1213.
(24) Campos, K. R.; Coleman, P. J.; Alvarez, J. C.; Dreher, S. D.; Garbaccio, R. M.; Terrett, N. K.; Tillyer, R. D.; Truppo, M. D.; Parmee, E. R. The importance of synthetic chemistry in the pharmaceutical industry. *Science* **2019**, *363*, No. eaat0805.
(25) Moghadam, F. A.; Hicks, E. F.; Sercel, Z. P.; Cusumano, A. Q.; Bartberger, M. D.; Stoltz, B. M. Ir-Catalyzed Asymmetric Allylic Alkylation of Dialkyl Malonates Enabling the Construction of Enantioenriched All-Carbon Quaternary Centers. *J. Am. Chem. Soc.* **2022**, *144*, 7983−7987.
(26) Ngamnithiporn, A.; Iwayama, T.; Bartberger, M. D.; Stoltz, B. M. Enantioselective synthesis of highly oxygenated acyclic quaternary center-containing building blocksviapalladium-catalyzed decarboxylative allylic alkylation of cyclic siloxyketones. *Chem. Sci.* **2020**, *11*, 11068−11071.
(27) Shockley, S. E.; Hethcox, J. C.; Stoltz, B. M. Enantioselective Synthesis of Acyclic alpha-Quaternary Carboxylic Acid Derivatives through Iridium-Catalyzed Allylic Alkylation. *Angew. Chem., Int. Ed.* **2017**, *56*, 11545−11548.
(28) Starkov, P.; Moore, J. T.; Duquette, D. C.; Stoltz, B. M.; Marek, I. Enantioselective Construction of Acyclic Quaternary Carbon Stereocenters: Palladium-Catalyzed Decarboxylative Allylic Alkylation of Fully Substituted Amide Enolates. *J. Am. Chem. Soc.* **2017**, *139*, 9615−9620.
(29) Trost, B. M.; Zhang, T.; Sieber, J. D. Catalytic asymmetric allylic alkylation employing heteroatom nucleophiles: a powerful method for C-X bond formation. *Chem. Sci.* **2010**, *1*, 427−440.
(30) Cheng, Q.; Tu, H. F.; Zheng, C.; Qu, J. P.; Helmchen, G.; You, S. L. Iridium-Catalyzed Asymmetric Allylic Substitution Reactions. *Chem. Rev.* **2019**, *119*, 1855−1969.
(31) He, Z.-T.; Hartwig, J. F. Enantioselective α-functionalizations of ketones via allylic substitution of silyl enol ethers. *Nat. Chem.* **2019**, *11*, 177−183.
(32) Ohmura, T.; Hartwig, J. F. Regio- and Enantioselective Allylic Amination of Achiral Allylic Esters Catalyzed by an Iridium−Phosphoramidite Complex. *J. Am. Chem. Soc.* **2002**, *124*, 15164−15165.
(33) Kim, S. W.; Schwartz, L. A.; Zbieg, J. R.; Stivala, C. E.; Krische, M. J. Regio- and Enantioselective Iridium-Catalyzed Amination of Racemic Branched Alkyl-Substituted Allylic Acetates with Primary and Secondary Aromatic and Heteroaromatic Amines. *J. Am. Chem. Soc.* **2019**, *141*, 671−676.
(34) Jung, W.-O.; Yoo, M.; Migliozzi, M. M.; Zbieg, J. R.; Stivala, C. E.; Krische, M. J. Regio- and Enantioselective Iridium-Catalyzed Amination of Alkyl-Substituted Allylic Acetates with Secondary Amines. *Org. Lett.* **2022**, *24*, 441−445.
(35) Trost, B. M.; Bunt, R. C.; Lemoine, R. C.; Calkins, T. L. Dynamic kinetic asymmetric transformation of diene monoepoxides: A practical asymmetric synthesis of vinylglycinol, vigabatrin, and ethambutol. *J. Am. Chem. Soc.* **2000**, *122*, 5968−5976.
(36) Pamies, O.; Margalef, J.; Canellas, S.; James, J.; Judge, E.; Guiry, P. J.; Moberg, C.; Backvall, J. E.; Pfaltz, A.; Pericas, M. A.; Dieguez, M. Recent Advances in Enantioselective Pd-Catalyzed Allylic Substitution: From Design to Applications. *Chem. Rev.* **2021**, *121*, 4373−4505.
(37) Trost, B. M.; Belletire, J. L.; Godleski, S.; Mcdougal, P. G.; Balkovec, J. M.; Baldwin, J. J.; Christy, M. E.; Ponticello, G. S.; Varga, S. L.; Springer, J. P. On the Use of the O-Methylmandelate Ester for Establishment of Absolute-Configuration of Secondary Alcohols. *J. Org. Chem.* **1986**, *51*, 2370−2374.
(38) Trost, B. M.; Machacek, M. R.; Tsui, H. C. Development of aliphatic alcohols as nucleophiles for palladium-catalyzed DYKAT reactions: Total synthesis of (+)-hippospongic acid A. *J. Am. Chem. Soc.* **2005**, *127*, 7014−7024.
(39) Trost, B. M.; Van Vranken, D. L. Asymmetric Transition Metal-Catalyzed Allylic Alkylations. *Chem. Rev.* **1996**, *96*, 395−422.
(40) Trost, B. M.; Crawley, M. L. Asymmetric Transition-Metal-Catalyzed Allylic Alkylations: Applications in Total Synthesis. *Chem. Rev.* **2003**, *103*, 2921−2944.
(41) Arnold, J. S.; Cizio, G. T.; Nguyen, H. M. Synthesis of alpha,alpha-Disubstituted Aryl Amines by Rhodium-Catalyzed Amination of Tertiary Allylic Trichloroacetimidates. *Org. Lett.* **2011**, *13*, 5576−5579.
(42) Kawatsura, M.; Uchida, K.; Terasaki, S.; Tsuji, H.; Minakawa, M.; Itoh, T. Ruthenium-Catalyzed Regio- and Enantioselective Allylic Amination of Racemic 1-Arylallyl Esters. *Org. Lett.* **2014**, *16*, 1470−1473.
(43) Mizuno, S.; Terasaki, S.; Shinozawa, T.; Kawatsura, M. Regioselective Construction of alpha,alpha-Disubstituted Allylic Amines by the Ruthenium-Catalyzed Allylic Amination of Tertiary Allylic Acetates. *Org. Lett.* **2017**, *19*, 504−507.
(44) Salman, M.; Xu, Y. Y.; Khan, S.; Zhang, J. J.; Khan, A. Regioselective molybdenum-catalyzed allylic substitution of tertiary allylic electrophiles: methodology development and applications. *Chem. Sci.* **2020**, *11*, 5481−5486.
(45) Zheng, W. H.; Sun, N.; Hou, X. L. Highly regio- and enantioselective palladium-catalyzed allylic alkylation and amination of dienyl esters with 1,1'-*P,N*-ferrocene ligands. *Org. Lett.* **2005**, *7*, 5151−5154.
(46) Hayashi, T.; Kawatsura, M.; Uozumi, Y. Retention of regiochemistry of allylic esters in palladium-catalyzed allylic alkylation in the presence of a MOP ligand. *J. Am. Chem. Soc.* **1998**, *120*, 1681−1687.
(47) Dubovyk, I.; Watson, I. D. G.; Yudin, A. K. Chasing the proton culprit from palladium-catalyzed allylic amination. *J. Am. Chem. Soc.* **2007**, *129*, 14172.
(48) Trost, B. M.; Osipov, M.; Dong, G. B. Palladium-Catalyzed Dynamic Kinetic Asymmetric Transformations of Vinyl Aziridines with Nitrogen Heterocycles: Rapid Access to Biologically Active Pyrroles and Indoles. *J. Am. Chem. Soc.* **2010**, *132*, 15800−15807.
(49) Khan, A.; Khan, S.; Khan, I.; Zhao, C.; Mao, Y. X.; Chen, Y.; Zhang, Y. J. Enantioselective Construction of Tertiary C-O Bond via Allylic Substitution of Vinylethylene Carbonates with Water and Alcohols. *J. Am. Chem. Soc.* **2017**, *139*, 10733−10741.
(50) Wang, Y. N.; Wang, B. C.; Zhang, M. M.; Gao, X. W.; Li, T. R.; Lu, L. Q.; Xiao, W. J. Hydrogen Bond Direction Enables Palladium-Catalyzed Branch- and Enantioselective Allylic Aminations and Beyond. *Org. Lett.* **2017**, *19*, 4094−4097.
(51) Arnold, J. S.; Nguyen, H. M. Rhodium-Catalyzed Dynamic Kinetic Asymmetric Transformations of Racemic Tertiary Allylic Trichloroacetimidates with Anilines. *J. Am. Chem. Soc.* **2012**, *134*, 8380−8383.
(52) Cai, A.; Guo, W.; Martínez-Rodríguez, L.; Kleij, A. W. Palladium-Catalyzed Regio- and Enantioselective Synthesis of Allylic Amines Featuring Tetrasubstituted Tertiary Carbons. *J. Am. Chem. Soc.* **2016**, *138*, 14194−14197.

https://doi.org/10.1021/jacs.3c04211
J. Am. Chem. Soc. 2023, 145, 19642−19654

(53) Hu, L.; Cai, A.; Wu, Z.; Kleij, A. W.; Huang, G. A Mechanistic Analysis of the Palladium-Catalyzed Formation of Branched Allylic Amines Reveals the Origin of the Regio- and Enantioselectivity through a Unique Inner-Sphere Pathway. *Angew. Chem., Int. Ed.* **2019**, *58*, 14694−14702.
(54) Shu, C. T.; Leitner, A.; Hartwig, J. F. Enantioselective allylation of aromatic amines after in situ generation of an activated cyclometalated iridium catalyst. *Angew. Chem., Int. Ed.* **2004**, *43*, 4797−4800.
(55) Wagaw, S.; Rennels, R. A.; Buchwald, S. L. Palladium-catalyzed coupling of optically active amines with aryl bromides. *J. Am. Chem. Soc.* **1997**, *119*, 8451−8458.
(56) Fischer, C.; Defieber, C.; Suzuki, T.; Carreira, E. M. Readily available [2.2.2]-bicyclooctadienes as new chiral ligands for Ir(I): Catalytic, kinetic resolution of allyl carbonates. *J. Am. Chem. Soc.* **2004**, *126*, 1628−1629.
(57) Wang, Z. Q.; Feng, C. G.; Xu, M. H.; Lin, G. Q. Design of C-2-symmetric tetrahydropentalenes as new chiral diene ligands for highly enantioselective Rh-catalyzed arylation of N-tosylarylimines with arylboronic acids. *J. Am. Chem. Soc.* 2007, *129* (17) 5336−+, DOI: 10.1021/ja0710914.
(58) Crabtree, R. H., *Organometallic Chemistry of the Transition Metals*, 4th ed.; 2005; pp 1−28.
(59) Bhat, V.; Welin, E. R.; Guo, X. L.; Stoltz, B. M. Advances in Stereoconvergent Catalysis from 2005 to 2015: Transition-Metal-Mediated Stereoablative Reactions, Dynamic Kinetic Resolutions, and Dynamic Kinetic Asymmetric Transformations. *Chem. Rev.* **2017**, *117*, 4528−4561.
(60) Mohr, J. T.; Moore, J. T.; Stoltz, B. M. Enantioconvergent catalysis. *Beilstein J. Org. Chem.* **2016**, *12*, 2038−2045.
(61) Steinreiber, J.; Faber, K.; Griengl, H. De-racemization of Enantiomers versus De-epimerization of Diastereomers-Classification of Dynamic Kinetic Asymmetric Transformations (DYKAT). *Chem. − Eur. J.* **2008**, *14*, 8060−8072.
(62) Guillaneux, D.; Zhao, S.-H.; Samuel, O.; Rainford, D.; Kagan, H. B. Nonlinear Effects in Asymmetric Catalysis. *J. Am. Chem. Soc.* **1994**, *116*, 9430−9439.
(63) Satyanarayana, T.; Abraham, S.; Kagan, H. B. Nonlinear Effects in Asymmetric Catalysis. *Angew. Chem., Int. Ed.* **2009**, *48*, 456−494.
(64) Geiger, Y.; Achard, T.; Maisse-Francois, A.; Bellemin-Laponnaz, S. Absence of Non-Linear Effects Despite Evidence for Catalyst Aggregation. *Eur. J. Org. Chem.* **2021**, *2021*, 2916−2922.
(65) Sorlin, A. M.; Mixdorf, J. C.; Rotella, M. E.; Martin, R. T.; Gutierrez, O.; Nguyen, H. M. The Role of Trichloroacetimidate To Enable Iridium-Catalyzed Regio-and Enantioselective Allylic Fluorination: A Combined Experimental and Computational Study. *J. Am. Chem. Soc.* **2019**, *141*, 14843−14852.
(66) Hughes, D. L.; Lloyd-Jones, G. C.; Krska, S. W.; Gouriou, L.; Bonnet, V. D.; Jack, K.; Sun, Y.; Mathre, D. J.; Reamer, R. A. Mechanistic studies of the molybdenum-catalyzed asymmetric alkylation reaction. *Proc. Natl. Acad. Sci. U. S. A.* **2004**, *101*, 5379−5384.
(67) Neel, A. J.; Hilton, M. J.; Sigman, M. S.; Toste, F. D. Exploiting non-covalent π interactions for catalyst design. *Nature* **2017**, *543*, 637−646.
(68) Lucet, D.; Le Gall, T.; Mioskowski, C. The chemistry of vicinal diamines. *Angew. Chem., Int. Ed.* **1998**, *37*, 2580−2627.
(69) Kotti, S. R. S. S.; Timmons, C.; Li, G. G. Vicinal diamino functionalities as privileged structural elements in biologically active compounds and exploitation of their synthetic chemistry. *Chem. Biol. Drug Des.* **2006**, *67*, 101−114.
(70) Lin, G. Q.; Xu, M. H.; Zhong, Y. W.; Sun, X. W. An advance on exploring N-tert-butanesulfinyl imines in asymmetric synthesis of chiral amines. *Acc. Chem. Res.* **2008**, *41*, 831−840.
(71) Zhu, Y. G.; Cornwall, R. G.; Du, H. F.; Zhao, B. G.; Shi, Y. Catalytic Diamination of Olefins via N-N Bond Activation. *Acc. Chem. Res.* **2014**, *47*, 3665−3678.
(72) Mwenda, E. T.; Nguyen, H. M. Enantioselective Synthesis of 1,2-Diamines Containing Tertiary and Quaternary Centers through Rhodium-Catalyzed DYKAT of Racemic Allylic Trichloroacetimidates. *Org. Lett.* **2017**, *19*, 4814−4817.
(73) Ibuka, T.; Mimura, N.; Aoyama, H.; Akaji, M.; Ohno, H.; Miwa, Y.; Taga, T.; Nakai, K.; Tamamura, H.; Fujii, N.; Yamamoto, Y. A thermodynamic preference of chiral N-methanesulfonyl and N-arenesulfonyl 2,3-cis-3-alkyl-2-vinylaziridines over their 2,3-trans-isomers: Useful palladium(0)-catalyzed equilibration reactions for the synthesis of (E)-alkene dipeptide isosteres. *J. Org. Chem.* **1997**, *62*, 999−1015.
(74) Murray, C. W.; Rees, D. C. The rise of fragment-based drug discovery. *Nat. Chem.* **2009**, *1*, 187−192.

https://doi.org/10.1021/jacs.3c04211
J. Am. Chem. Soc. 2023, 145, 19642−19654